Simulation of Control System for a Half-Car Suspension System for Passenger Vehicle Application by Designing an LQR Controller

Walelign Wudu Bezabh, Ayitenew Mogninet Getaneh, Mequanint Birhan

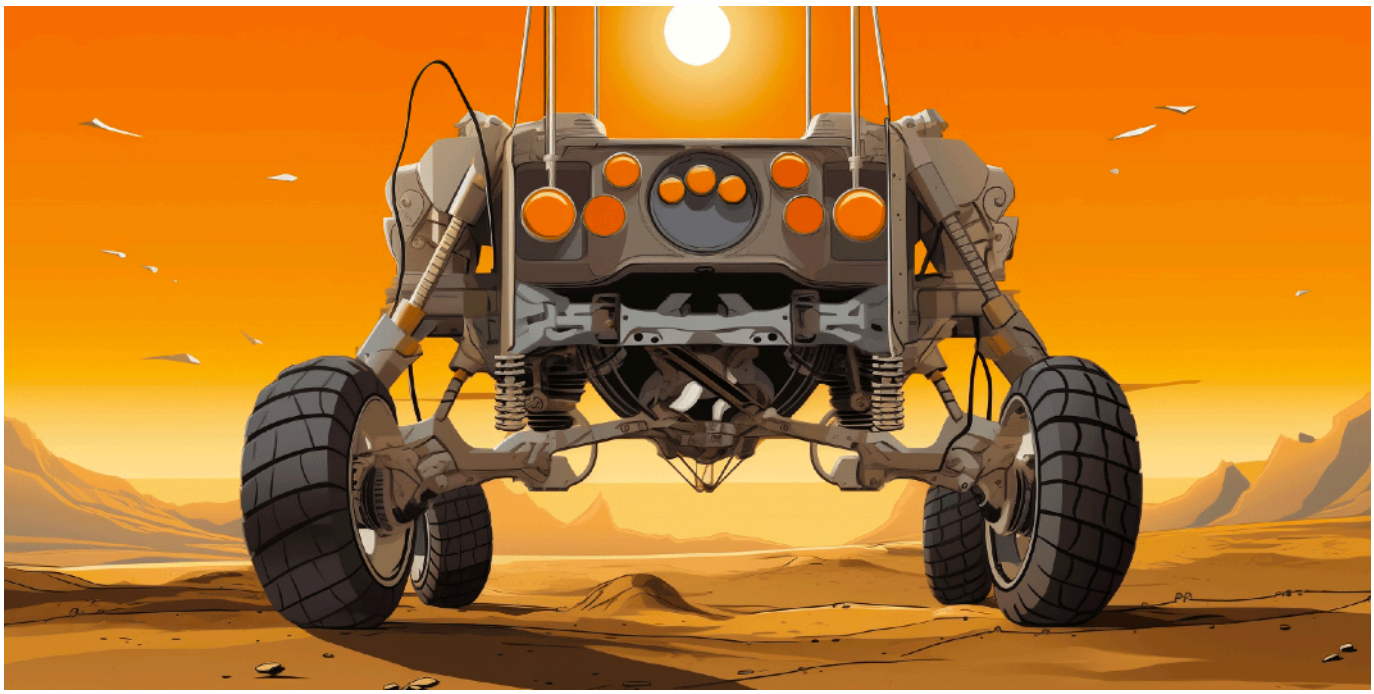

Preprint v1

Nov 6, 2023

https://doi.org/10.32388/SGEORJ

Simulation of Control System for a Half-Car Suspension System for Passenger Vehicle Application by Designing an LQR Controller

Walelign Wudu Bezabh*, Ayitenew Mogninet Getaneh, Mequanint Birhan
Department of Mechanical Engineering, Mizan Tepi University, Tepi Illubabur, Ethiopia

**Corresponding Author's e-mail: walelign@mtu.edu.et*

Abstract: The constantly growing topic of inventive vehicle system design is of interest to researchers. The difficulty stems from the ongoing requirement for advancement in vehicle handling, ride comfort, and driving dynamics. Based on a control method for ride comfort and vehicle handling, this study has proposed a mathematical model for a 4-DOF half-car active suspension system (ASS) employing an LQR (Linear Quadratic Regulator) controller. The task is simulated using MATLAB/Simulink software. The unsprung masses of the wheels' heave displacements, the vehicle's pitching dynamics, and the sprung masses of its body's heave displacements are the regulated parameters. Compared to the antiquated passive suspension technology, its performance is superior (PSS). The simulation uses two bumpy sinusoidal roads and a random road input. Finally, the performance of the suggested controller was demonstrated using simulation software. The results of the simulation demonstrate that this study has improved its modeling and control capabilities.

Keywords: Active suspension, LQR, 4-DOF, MATLAB/Simulink.

1. Introduction

Designing new vehicle systems is a rapidly expanding profession that attracts the attention of researchers. The ever-increasing improvement needs related to driving dynamics, ride comfort, and vehicle handling, however, pose a difficulty. Environmental protection and fuel efficiency have also become major considerations for customers when purchasing a new vehicle. More efficient drive dynamics control technologies, such as active suspension systems, can be developed to satisfy these needs. The primary function of the suspension system is to maintain constant wheel contact with the road to provide road holding and to isolate a vehicle body from road irregularities during braking, cornering, and accelerating to improve driving comfort and safety [1, 2, 3]. In order to prevent suspension movements from resulting in insufficient tire-to-road contact, the term "vehicle handling regulation" is used. A vehicle's body and wheels are connected by a suspension system, which is made up of a number of springs, dampers, and connections [4, 5]. While the

damper distributes this energy and aids in damping the oscillations, the spring transports the body's mass by storing energy and helping to separate the body from road disturbances. The three basic types of damping suspension systems—a passive suspension system (PSS), a semi-active suspension system (SASS), and an active suspension system (ASS)—are frequently listed in vehicle categorization systems [6, 14, 15]. The least complicated suspension system, the passive suspension, has many benefits. The limitation of passive suspension, however, is its inability to eliminate undesired vibration brought on by anomalies in the road [7, 8]. The semi-active suspension thus utilizes a traditional spring and externally controlled damper to produce better performance outcomes [9]. Active suspension systems offer superior handling, road feel, and responsiveness in comparison to passive systems, as well as roll stability and safety with the actuator's force. Active suspension systems can also adjust their dynamic characteristics in response to changing road conditions in real-time.

Based on the information from the many sensors connected to it, the actuator force provides the system with an appropriate amount of control force. To improve the performance of the active suspension system, researchers have suggested LQR control methods. Only a few researchers have focused on the entire motion control of a half-vehicle, even though many independent suspension experiments have concentrated on simpler two-degree-of-freedom quarter-car models. Despite the fact that there have recently been a few studies on full dynamic management of the vehicle, this study was carried out using a static dynamics model, and the inputs for road disturbance are sinusoidal and random-type road inputs. The objective of the automotive suspension system is to regulate the dynamic tire load with sufficient suspension working space to maximize the vehicle's stability and safety, as well as to isolate the effect of road surface disturbances on passengers to boost ride comfort. Therefore, the half-dynamic model of a vehicle and controller design were the focus of this research to address the aforementioned issues. Various vehicle speeds (20 km/h, 40 km/h, 60 km/h, and 80 km/h) were used for improved accuracy. As a result, a controller was created for a chosen car model that has sprung and unsprung mass dynamics suspension systems.

2. Mathematical Modeling

In this section, a comprehensive mathematical model of the active and passive car suspension systems is developed for comparison purposes. As a result, the mathematical equation of the vehicle model under a dynamic situation is presented in the following part. The chosen model is

described in the table below for numerical purposes.

Table 1. The model's characteristic variables

Model	**Measuring Unit**	**Numerical Value**
m_s: Vehicle body sprung mass	K g	1794.4
m_{uf}: Unsprung mass at the front vehicle body	K g	87.15
m_{ur}: Unsprung mass at the rear vehicle body	K g	140.14
c_{sf}: Front suspension damper coefficient	N s/m	1190
c_{sr}: Rear suspension damper coefficient	N s/m	1000
k_{sf}: Stiffness coefficient at the front suspension	N /m	66824
k_{sr}: Stiffness coefficient at Rear suspension	N /m	18615
k_{uf}: Stiffness coefficient at the front wheel	N /m	101115
k_{ur}: Stiffness coefficient at the rear wheel	N /m	101115
J_s: Pitch Axis Moment of Inertia	K g m^2	3443.05
L_1: Length between the rear wheel and center of gravity	M	1.72
L_2: Length between the front wheel and center of gravity	M	1.27
U_1: Front actuator input	—	—
U_2: Rear actuator input	—	—

Table 2. Variables describing the model

Model	**Measuring Unit**
x_s: Chassis vertical displacement at center of gravity	M
x_{sf}: Front chassis vertical displacement	M

Model	Measuring Unit
x_{sr}: Rear chassis vertical displacement	M
x_{uf}: Front wheels vertical displacement	M
x_{ur}: Rear wheels vertical displacement	M
x_{wf}: Front road profiles	M
x_{wr}: Rear road profiles	M

2.1. Mathematical Modeling of Active Suspension System (ASS)

The state variable in the active suspension system can be controlled through a controller, which was selected for this study.

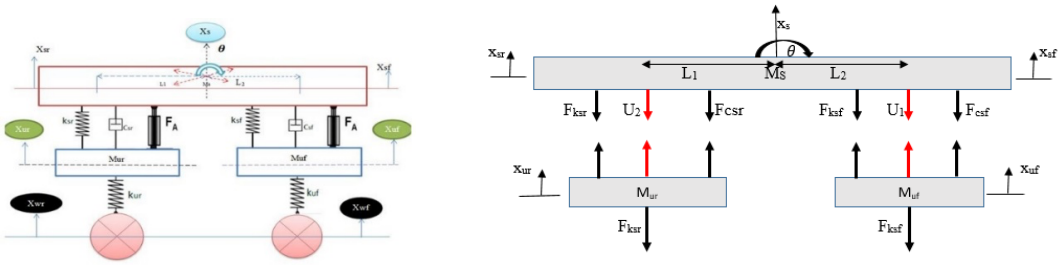

Figure 1. Model of half-car and Free Body Diagram (FBD) of 4-DOF sprung

The model equation of a sprung mass on the vertical motion at the center of gravity point

$$\ddot{x}_s = \frac{-\begin{bmatrix} c_{sf}\left(\dot{x}_{sf} - \dot{x}_{uf} - L_2\dot{\theta}\right) + k_{sf}\left(x_{sf} - x_{uf} - L_2\theta\right) + c_{sr}\left(\dot{x}_{sr} - \dot{x}_{ur} + L_1\dot{\theta}\right) \\ + k_{sr}\left(x_{sr} - x_{ur} + L_1\theta\right) - F_{AF} - F_{AR} \end{bmatrix}}{m_s} \quad (1)$$

$$\ddot{\theta} = \frac{\begin{bmatrix} L_2 c_{sf}\left(\dot{x}_{sf} - \dot{x}_{uf} - L_2\dot{\theta}\right) + L_2 k_{sf}\left(x_{sf} - x_{uf} - L_2\theta\right) - L_1 c_{sr}\left(\dot{x}_{sr} - \dot{x}_{ur} + L_1\dot{\theta}\right) \\ - L_1 k_{sr}\left(x_{sr} - x_{ur} + L_1\theta\right) + L_2 F_{AF} - L_1 F_{AR} \end{bmatrix}}{J} \quad (2)$$

$$\ddot{x}_{ur} = \frac{\left[c_{sr}\left(\dot{x}_{sr} - \dot{x}_{ur} + L_1\dot{\theta}\right) + k_{sr}\left(x_{sr} - x_{ur} + L_1\theta\right) - k_{ur}\left(x_{ur} - x_{wr}\right) - F_{AR}\right]}{m_{ur}} \quad (3)$$

$$\ddot{x}_{uf} = \frac{\left[c_{sf}\left(\dot{x}_{sf} - \dot{x}_{uf} + L_2\dot{\theta}\right) + k_{sf}\left(x_{sf} - x_{uf} + L_2\theta\right) - k_{uf}\left(x_{uf} - x_{wf}\right) - F_{Af}\right]}{m_{uf}} \quad (4)$$

For control purposes, the state variable should be linearly independent. Let's assume that the pitching dynamics in the forward direction are positive.

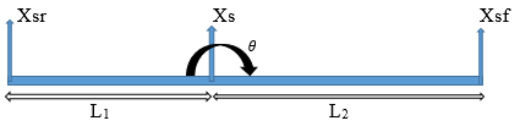

, From geometry $\theta = \dfrac{x_{sr} - x_{sf}}{L}$, $x_s = \dfrac{L_2 x_{sr} + L_1 x_{sf}}{L}$

2.2. State-space Model for an Active Suspension System

The model can be written in the following state-space form.

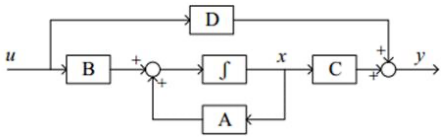

Figure 2. Block diagram for state-space representation

$$\dot{x}(t) = Ax(t) + BU$$
$$y = Cx(t) + DU \tag{5}$$

$$x_{sr} = x_1, \dot{x}_{sr} = x_2, x_{ur} = x_3, \dot{x}_{ur} = x_4, x_{sf} = x_5, \dot{x}_{sf} = x_6, x_{uf} = x_7, \dot{x}_{uf} = x_8$$

Let $$y_1 = \frac{L_2 + L}{L}, y_2 = \frac{L_1 + L}{L}, y_3 = \frac{L_2}{L}, y_4 = \frac{L_1}{L}, z_4 = \frac{L^2{}_1 m_s + j}{m_s j}$$

$$z_1 = \frac{L_1 L_2 m_s - J - L L_2 m_s}{m_s}, z_2 = \frac{L_1 m_s L - L^2{}_1 m_s - j}{m_s j},$$

$$z_3 = \frac{L_1 L_2 m_s - j}{m_s j}, z_4 = \frac{L_1{}^2 m_s + j}{m_s j}$$

$$\dot{x}_2 = z_3 \begin{pmatrix} c_{sf}\left(y_1 x_6 - y_3 x_2 - x_8\right) \\ + k_{sf}\left(y_1 x_5 - y_3 x_1 - x_7\right) \end{pmatrix} - z_4 \begin{pmatrix} c_{sr}\left(y_2 x_2 - y_4 x_6 - x_4\right) \\ + k_{sr}\left(y_2 x_1 - y_4 x_5 - x_3\right) \end{pmatrix} + z_3 u_1 - z_4 u_2 \tag{6}$$

$$\dot{x}_4 = \frac{c_{sr}\left(y_2 x_2 - y_4 x_6 - x_4\right) + k_{sr}\left(y_2 x_1 - y_4 x_5 - x_3\right) - k_{ur}\left(x_3 - x_{wr}\right) - u_2}{m_{ur}} \tag{7}$$

$$\dot{x}_6 = z_1 \begin{pmatrix} c_{sf}\left(y_1 x_6 - y_3 x_2 - x_8\right) \\ + k_{sf}\left(y_1 x_5 - y_3 x_1 - x_7\right) \end{pmatrix} + z_2 \begin{pmatrix} c_{sr}\left(y_2 x_2 - y_4 x_6 - x_4\right) \\ + k_{sr}\left(y_2 x_1 - y_4 x_5 - x_3\right) \end{pmatrix} + z_1 u_1 - z_2 u_2 \tag{8}$$

$$\dot{x}_8 = \frac{c_{sf}\left(y_1 x_6 - y_3 x_2 - x_8\right) + k_{sf}\left(y_1 x_5 - y_3 x_1 - x_7\right) - k_{uf}\left(x_7 - x_{wf}\right) - u_1}{m_{uf}} \tag{9}$$

The state-space equations of the suspension system for the design of the LQR control are as follows, based on the physical model of the vehicle in Figure 2.

Let

$$\lfloor A_1 \rfloor = [0 \quad 1 \quad 0 \quad 0 \quad 0 \quad 0 \quad 0 \quad 0], \qquad \lfloor A_3 \rfloor = [0 \quad 0 \quad 0 \quad 1 \quad 0 \quad 0 \quad 0 \quad 0]$$

$$\lfloor A_5 \rfloor = [0 \quad 0 \quad 0 \quad 0 \quad 0 \quad 1 \quad 0 \quad 0], \qquad \lfloor A_7 \rfloor = [0 \quad 0 \quad 0 \quad 0 \quad 0 \quad 0 \quad 0 \quad 1]$$

$$\lfloor A_2 \rfloor = \begin{bmatrix} -z_3 * k_{sf} * y_3 - z_4 * k_{sr} * y_2 \\ -z_3 * c_{sf} * y_3 - z_4 * c_{sr} * y_2 \\ z_4 * k_{sr} \\ z_4 * c_{sr} \\ z_3 * k_{sf} * y_1 + z_4 * k_{sr} * y_4 \\ z_3 * c_{sf} * y_1 + z_4 * c_{sr} * y_4 \\ -z_3 * k_{sf} \\ -z_3 * c_{sf} \end{bmatrix}^T, \quad \lfloor A_6 \rfloor = \begin{bmatrix} z_2 * k_{sr} * y_2 - z_1 * k_{sf} * y_3 \\ z_2 * c_{sr} * y_2 - z_1 * c_{sf} * y_3 \\ -z_2 * k_{sr} \\ -z_2 * c_{sr} \\ z_1 * k_{sf} * y_1 - z_4 * k_{sr} * y_4 \\ z_1 * c_{sf} * y_1 - z_2 * c_{sr} * y_4 \\ -z_1 * k_{sf} \\ -z_1 * c_{sf} \end{bmatrix}^T$$

$$\lfloor A_4 \rfloor = \begin{bmatrix} \frac{y_2 * k_{sr}}{m_{ur}} & \frac{y_2 * c_{sr}}{m_{ur}} & \frac{-k_{sr} - k_{ur}}{m_{ur}} & \frac{-c_{sr}}{m_{ur}} & \frac{-y_4 * k_{sr}}{m_{ur}} & \frac{-y_4 * c_{sr}}{m_{ur}} & 0 & 0 \end{bmatrix}$$

$$\lfloor A_8 \rfloor = \begin{bmatrix} \frac{-y_3 * k_{sf}}{m_{uf}} & \frac{-y_3 * c_{sf}}{m_{uf}} & 0 & 0 & \frac{y_1 * k_{sf}}{m_{uf}} & \frac{y_1 * c_{sf}}{m_{uf}} & \frac{-k_{sf} - k_{uf}}{m_{uf}} & \frac{-c_{sf}}{m_{uf}} \end{bmatrix}, \quad [G] = \begin{bmatrix} u_1 & u_2 \end{bmatrix}^T$$

$$[B] = \begin{bmatrix} 0 & z_3 & 0 & 0 & 0 & z_1 & 0 & -1/m_{uf} \\ 0 & -z_4 & 0 & -1/m_{ur} & 0 & -z_2 & 0 & 0 \end{bmatrix}^T, \quad [G] = \begin{bmatrix} 0 & 0 & 0 & 0 & 0 & 0 & 0 & k_{uf}/m_{uf} \\ 0 & 0 & 0 & k_{ur}/m_{ur} & 0 & 0 & 0 & 0 \end{bmatrix}^T,$$

3. Control System Design

The objective of any control system is to identify deviations between the output and the target value and then make the required adjustments to get the output back on track. In this study, PID and LQR controllers are used, which are based on their design specifications.

3.1. LQR Controller

The minimization of costs or objective functions that are quadratic in both the state and the control, and the generation of performance indices, are all components of the linear quadratic regulator, a particular type of optimal control problem [10, 16]. The aim of optimum control was to find a control vector (U1 and U2) that drives the behavior of the dynamic system to the desired final state while also fulfilling the physical constraints.

$$J = \int_0^\infty \left(x^T Q_x + U^T R U \right) dt \tag{10}$$

Both Q and R are positive definite Hermitian or real symmetric matrices, with Q being positive-definite (or positive-semi-definite). The matrices Q and R are selected to minimize the cost function "J." The state feedback gain matrix K is used to define the value of the feedback control vector 'u' as -Kx. In this study, the built-in MATLAB program "K = lqr (A, B, Q, R)" is used to determine the ideal value of K. The values of the Q and R matrices are selected iteratively until the desired outcomes for the given suspension parameters are attained. The best value of K is discovered as:

K =

1.0e+03 *

Columns 1 Column 8

0.1866 -0.0654 -1.5035 -0.0172 -2.2534 -0.9812 2.9981 -0.8697

-2.1776 -1.1260 2.8158 -0.9720 3.5098 0.0176 -1.1198 -0.0213

4. Simulation and Result Analysis

To assess the efficacy of the suggested LQR controller, numerical simulations are performed on the 4-DOF half-vehicle model ASS in this section. The parameters of the vehicle are shown in Table 1 for modeling purposes. The MATLAB/Simulink software is used to run the simulation.

4.1. Comparative Performance of ASS to PSS Simulation for Two Bump Sinusoidal Road Input

These simulations are intended to compare the performance of the ASS and PSS on two different bump road profiles. Two instances of bump sinusoidal road profiles are shown below, where [9, 13] is the value, and h is the amplitude of the bump. It is discovered that a sinusoidal bump with an 8 Hz frequency had two bumps.

$$x_{wf(t)} = \begin{Bmatrix} h(1-\cos(8\pi t)), 0.5 \le t \le 0.75\,\text{sec} \\ h\left(\frac{1-\cos(8\pi t)}{2}\right), 3.5 \le t \le 3.75\,\text{sec} \\ 0, otherwise \end{Bmatrix}, \quad x_{wr(t)} = \begin{Bmatrix} h(1-\cos(8\pi t)), 3 \le t \le 3.25\,\text{sec} \\ h\left(\frac{1-\cos(8\pi t)}{2}\right), 7.25 \le t \le 7.5\,\text{sec} \\ 0, otherwise \end{Bmatrix} \tag{11}$$

Equation 11 represents an input disturbance for the front and for the rear wheel.

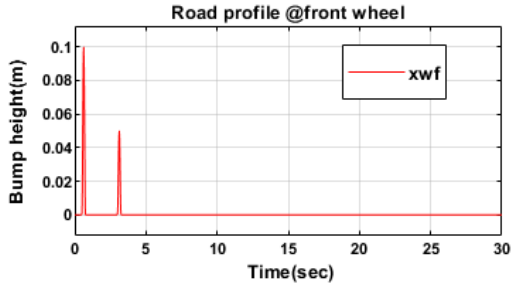

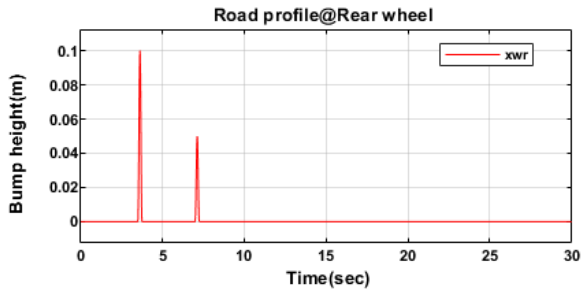

Figure 4. Front-wheel and Rear wheel two bump expected road profile simulation

The classification of road roughness for this study is based on ISO. The type B (good) and type C (average) random road inputs are designed for four vehicle operating speeds, as explained below. These speeds–20 km/h, 40 km/h, 60 km/h, and 80 km/h–help illustrate the effects of road roughness and vehicle speeds, as well as the increase in road handling and passenger ride quality. Using equation 12, the power spectral density for each vehicle's speed is computed.

$$x_{w(t)} = \sqrt{k}\int w(t)dt \tag{12}$$

Where v is the vehicle speed, w(t) is white noise, k is the spectral density constant, G(no) value for B and C type road input $=16 * 10^{-6}m^3$, $64 * 10^{-6}m^3$ respectively. [12]

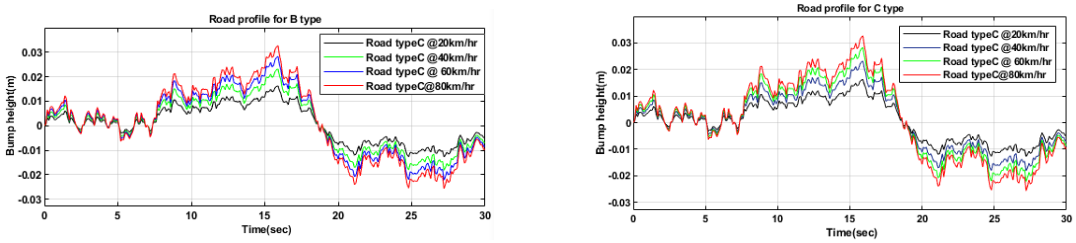

Figure 5. Random road profile types B and C at selected vehicle speed simulated respectively.

4.2. Performance Analysis and Comparison of the Suspension System with LQR Controller

In this section, the LQR controller is applied simultaneously, and the performance comparison is shown in the following graph, obtained from MATLAB Simulink.

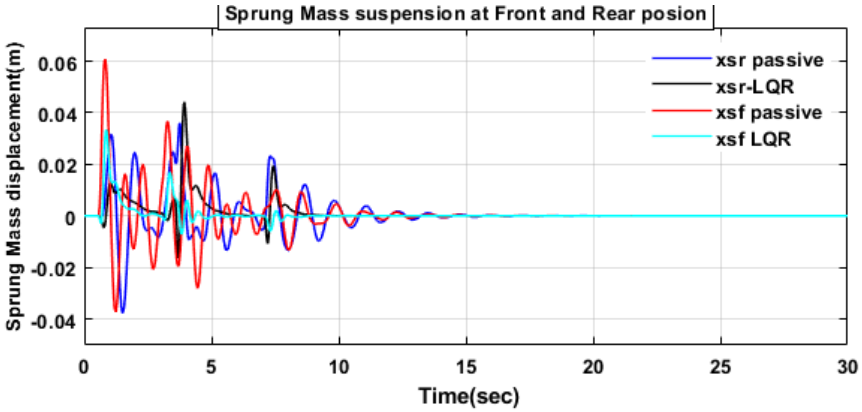

Figure 6. Displacement of the vehicle body at rear and front positions.

The outcome of the vehicle's body displacement output for the car's rear and front suspension system, both passive and active. From the simulation, the vehicle's vertical displacement at the positive peak values reached 0.06 m for passive and 0.031 m for LQR.

In the new design, the controller responds when the odd thing happens before it reaches the passengers.

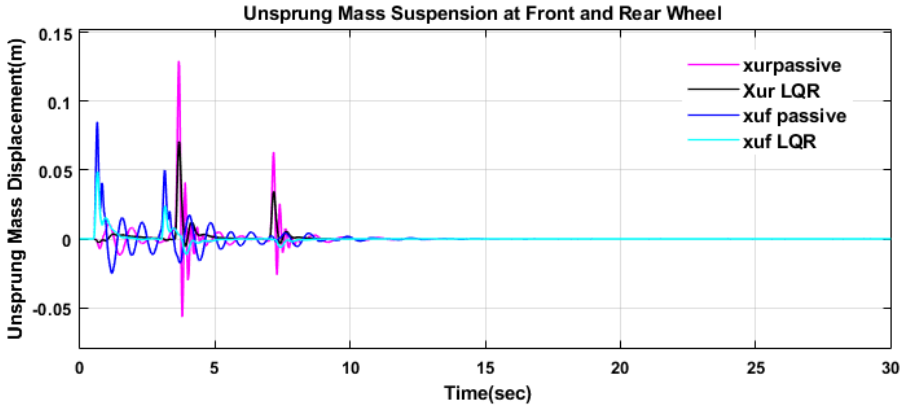

Figure 7. Front and rear wheels displacement comparison.

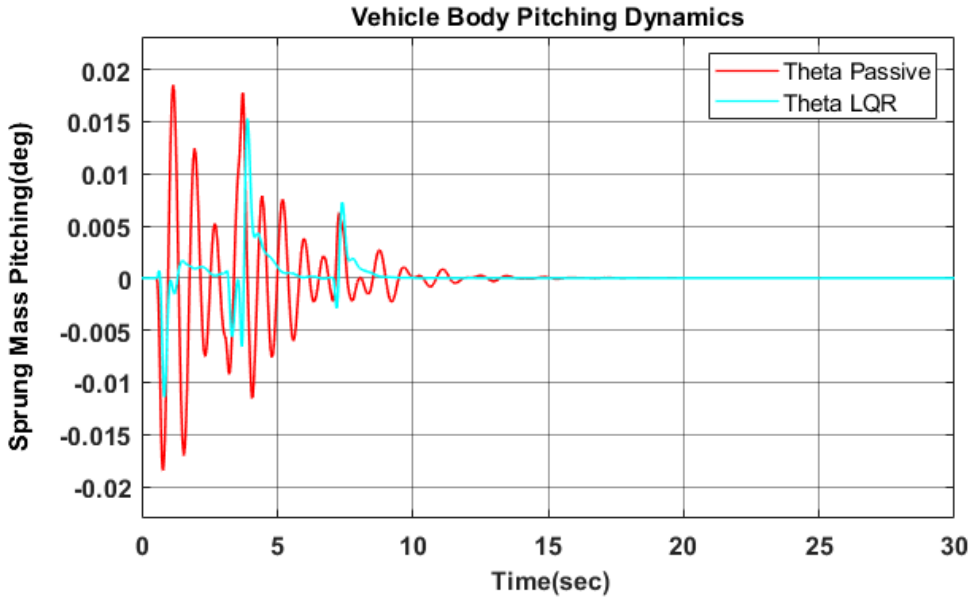

Figure 8. Vehicle pitching dynamics on the lateral direction

The pitch degree of bump disturbance for passive and active suspension systems is shown in Figure 8. The active system with an LQR controller provides a better reaction to the road profile with less vibration and error. As the graph shows, the LQR controller gives a response and stabilizes the system with minimal pitch in the lateral direction, whereas in passive suspension, the pitch reaches a maximum compared to the active system.

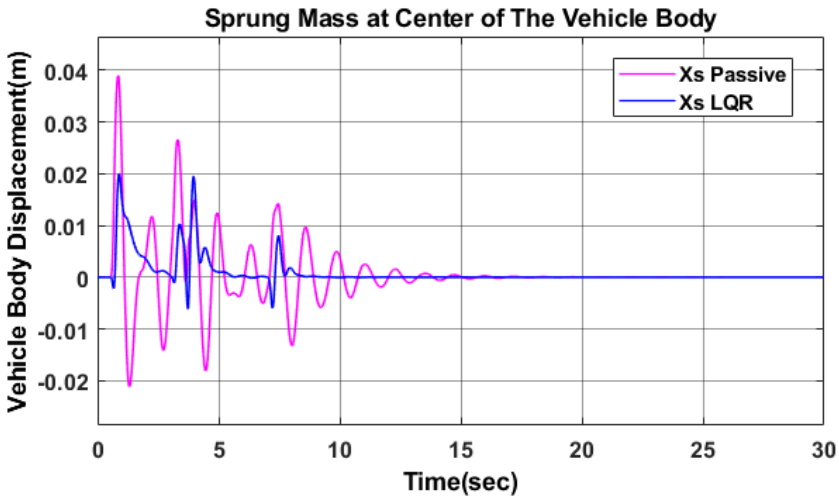

Figure 9. Sprung mass displacement

Figure 9 shows that the suspension system with an LQR controller improves ride quality by reducing overshoot and achieving a small steady-state error in response to the selected road disturbance. The suspension without control exhibits poorer traction compared to the peak-to-peak value of the new design.

4.3. Simulation Results of the Model on Band C Type Random Road Input at 20, 40, 60, and 80 km/hr Vehicle Speeds

When traveling at vehicle speeds of 20, 40, 60, and 80 km/hr, the performance of PSS and active suspension systems with an LQR controller is compared for the states of the vehicle body heave at the center of gravity, front-wheel displacement, rear-wheel displacement, and pitching displacements on B and C class random road inputs. The graph depicts the relationship between the road input and the simulation of vehicle speed in this segment.

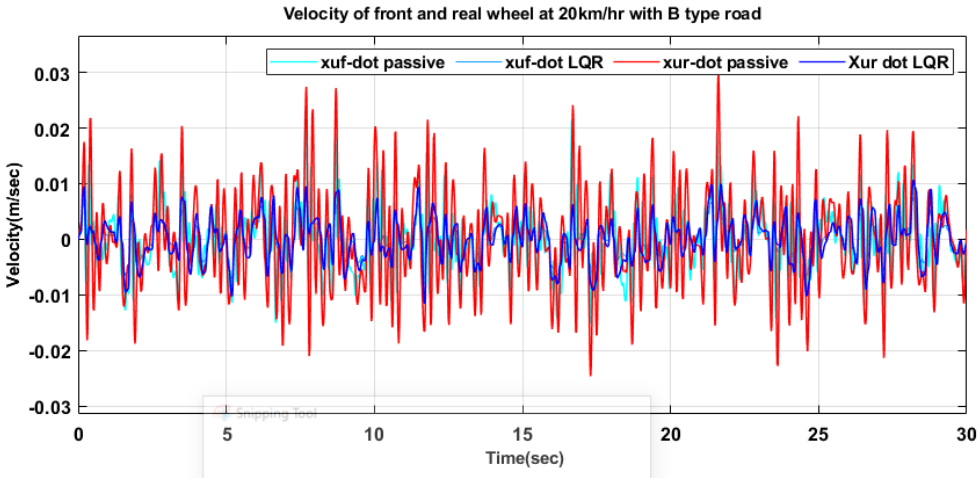

Figure 10. Front and rear wheels velocity at 20 km/hr

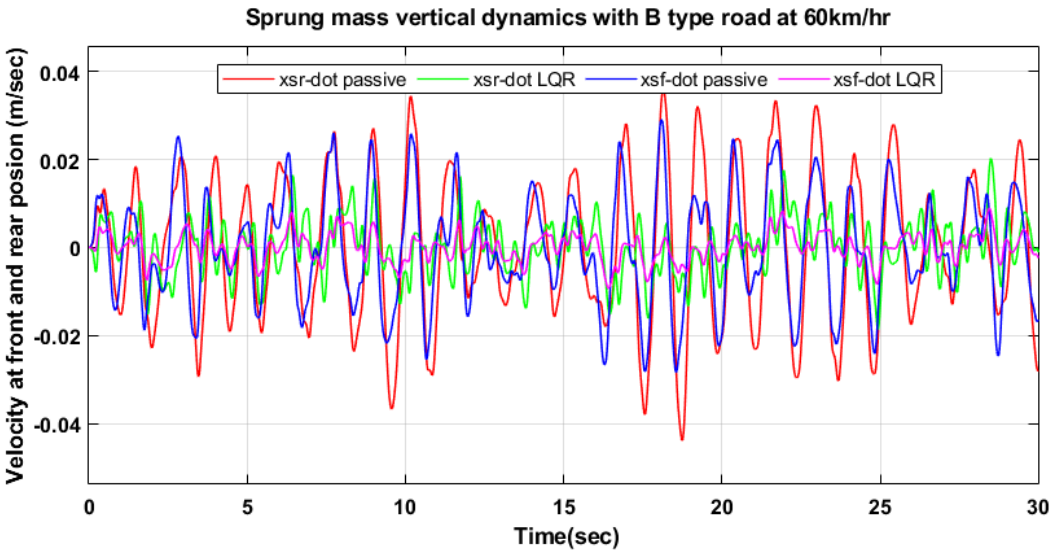

Figure 11. Vehicle body velocity at 60 km/hr

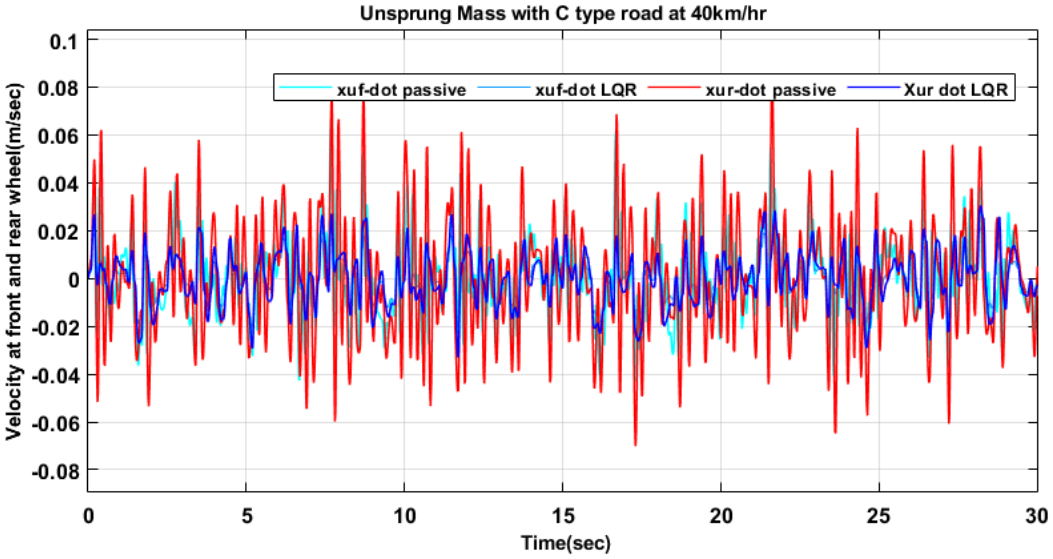

Figure 12. Front and rear wheels Velocity at 40 km/hr

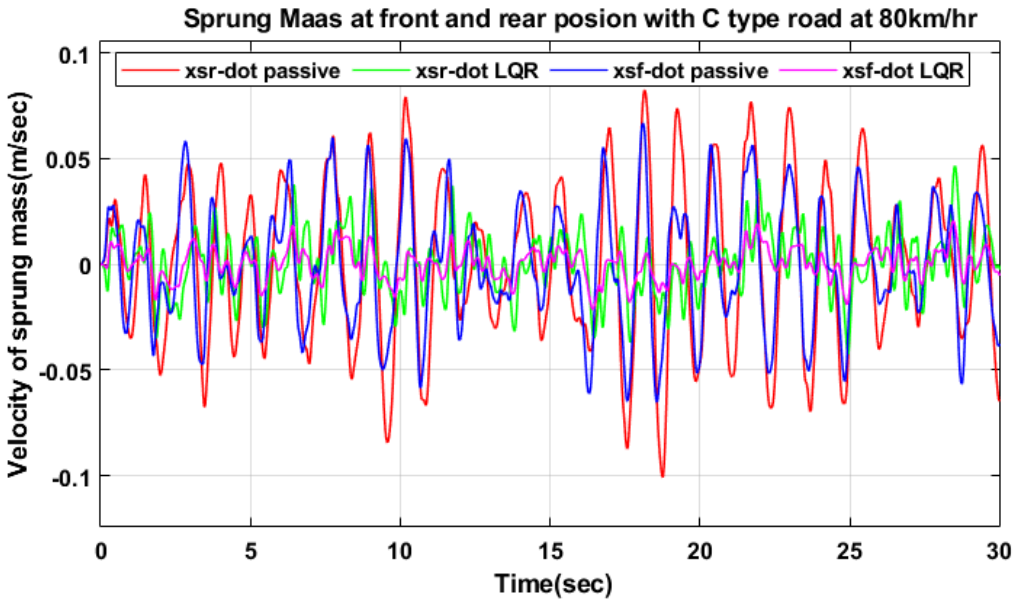

Figure 13. Vehicle body Velocity at Front and rear position at 80 km/hr

Figures 10, 11, 12, and 13 show that by applying an LQR controller with random road inputs in the half-vehicle model, the velocity of the sprung mass and unsprung mass around the x and y-*axes* of the analyzed model was reduced in terms of peak-to-peak value, and settling time is faster as well.

5. Conclusion

This work focused on the modeling and control of a passenger half-car suspension system. A mathematical model for a linear 4-DOF car suspension system was built and derived under dynamic conditions. A chosen controller was then used after the dynamic model had been created, and its performance was evaluated at various vehicle speeds while being subjected to input disturbances from bumpy roads. The effectiveness and performance of the controller were verified by simulation using MATLAB/Simulink.

- In the vertical direction, peak-to-peak, the active suspension system (ASS) with an LQR controller improves performance. Additionally, sprung masses tilting in the lateral direction improved.
- The new design with an LQR controller successfully controls the dynamic effect in both expected and random road inputs. In the Simulink graph, the controller provides improved comfort in the vertical and lateral directions and good handling at the two wheels.

The research demonstrates that in controlled ASS, sprung and unsprung mass heave displacements have amplitudes and settling times that are much less than in uncontrolled passive suspension systems (PSS). Overall, the dynamic modeling of the LQR controller of the ASS is efficient and produces good outcomes.

Reference

[1] Avesh M, Srivastava R. (2012). Modeling simulation and control of active suspension system in Matlab Simulink environment. In Students Conference on Engineering and Systems 2012 (pp. 1-6). IEEE.

[2] Khan MA, Abid M, Ahmed N, Wadood A, Park H. (2020). Nonlinear control design of a half-car model using feedback linearization and an LQR controller. *Applied Sciences, 10*(9), 3075.

[3] Fischer D, Isermann R. (2004). Mechatronic semi-active and active vehicle suspensions. *Control Engineering Practice, 12*(11), 1353-1367.

[4] Lauwerys C, Swevers J, Sas P. (2005). Robust linear control of an active suspension on a quarter car test-rig. *Control Engineering Practice, 13*(5), 577-586.

[5] Chen H, Guo KH. (2005). Constrained H∞ control of active suspensions: an LMI approach. *IEEE Transactions on Control Systems Technology, 13*(3), 412-421.

[6] Sharkawy AB. (2005). Fuzzy and adaptive fuzzy control for the automobiles' active suspension system. *Vehicle System Dynamics, 43*(11), 795-806.

[7] Sun J, Yang Q. (2009). Compare and analysis of passive and active suspensions under random road excitation. In IEEE International Conference on Automation and Logistics 2009 (pp. 1577-1580). IEEE.

[8] Antehunegn Y, Belete M. (2020). Control of 8 DOF vehicle model suspension system by designing Second order SMC Controller. *Global Scientific Journals, 8*(12).

[9] Ahmed AE, Ali AS, Ghazaly NM, Abd el-Jaber GT. (2015). PID controller of active suspension system for a quarter car model. *International Journal of Advances in Engineering & Technology, 8*(6), 899.

[10] Ajasa AA, Sebiotimo AA. The use of Matlab in the Solution of Linear Quadratic Regulator (LQR) Problems.

[11] Naidu DS. (2002). Optimal control systems. CRC press.

[12] Gandhi P, Adarsh S, Ramachandran KI. (2017). Performance analysis of half car suspension model with 4 DOF using PID, LQR, FUZZY and ANFIS controllers. *Procedia Computer Science, 115*, 2-13.

[13] Hasbullah F, Faris WF. (2010). A comparative analysis of LQR and fuzzy logic controller for active suspension using half car model. In 11th International Conference on Control Automation Robotics & Vision 2010 (pp. 2415-2420). IEEE.

[14] Nagarkar, M. P., and GJ Vikhe Patil. (2012). Performance analysis of quarter car active suspension system: LQR and H∞ control strategies. In Third International Conference on Computing, Communication and Networking Technologies (ICCCNT'12). IEEE.

[15] Agharkakli, Abdolvahab, Ghobad Shafiei Sabet, and Armin Barouz. (2012). Simulation and analysis of passive and active suspension system using quarter car model for different road profile. *International Journal of Engineering Trends and Technology, 3*(5), 636-644.

[16] Okyere, Emmanuel, et al. (2019). LQR controller design for quad-rotor helicopters. *The Journal of Engineering, 2019*(17), 4003-4007.